

Electronic Supplementary Information (ESI):

A precursor route to porous ZnO nanotubes with superior gas sensing properties

Pei-Pei Wang^a, Qi Qi^a, Xiaoxin Zou^{*ac}, Jun Zhao^a, Rui-Fei Xuan^{ab} and Guo-Dong Li^{*a}

*^aState Key Laboratory of Inorganic Synthesis and Preparative Chemistry, Jilin
University, Changchun 130012, China*

*^bCollege of Materials Science and Engineering, China University of Mining and
Technology, Xuzhou 221116, China*

*^cDepartment of Chemistry and Chemical Biology, Rutgers, The State University of
New Jersey, NJ 08854, USA*

* Corresponding author. Guo-Dong Li and Xiaoxin Zou, Tel/Fax: 86-431-85168318,
86-431-85168624
E-mail address: G. D. Li, lgd@jlu.edu.cn; X. Zou, chemistryzouxx@gmail.com

1. Experimental

1.1 Materials

Zinc acetate dihydrate, thiourea, cyclohexylamine (CHA) are purchased from Beijing Chemical Factory. Corresponding gas sensing reagents such as methanol, ethanol and formaldehyde solution are also purchased from Beijing Chemical Factory. All of the reagents are of analytic grade and used as received without further purification.

1.2 Preparation of ZnS-CHA composite nanorods

In a typical synthesis, zinc acetate dihydrate (0.32 g, 1.5 mmol) as the zinc source and thiourea (0.255 g, 3 mmol) as the sulfur source were added to CHA (40 mL) and stirred vigorously at room temperature. The mixture was sealed and heated at 120 °C for 20 h in a 50 mL PTFE-lined stainless steel autoclave. The white ZnS-CHA precipitate was obtained after cooling down to room temperature, which was washed several times with ethanol and dried at 60 °C for 6 h. The yield of ZnS-CHA was nearly 100% on the basis of the zinc source used.

1.3 Synthesis of porous ZnO nanotubes

Porous ZnO nanotubes were prepared by calcining the as-synthesized ZnS-CHA nanocomposite at 500 °C for 5 h in air.

1.4 General characterization

The X-ray diffraction (XRD) analysis of the products were recorded on a Rigaku D/Max 2550 X-ray diffractometer using Cu K α radiation ($\lambda = 1.5418 \text{ \AA}$). The scanning electron microscopic (SEM) images were performed on a JEOL JSM 6700F electron microscope. The transmission electron microscopic (TEM) and high-resolution TEM (HRTEM) images were taken on a FEI Tecnai G2S-Twin microscope. The X-ray photoelectron spectroscopy (XPS) was obtained on an ESCALAB 250 X-ray photoelectron spectrometer with a monochromated X-ray source (Al KR $h\nu = 1486.6 \text{ eV}$). The FT-IR spectra were obtained on a Bruker IFS 66v/S FTIR spectrometer. The thermogravimetric (TG) analysis for ZnS-CHA was conducted in air on a NETZSCH STA 449C TG thermal analyzer from 25 to 800 °C at a heating rate of 10 °C min⁻¹. Nitrogen adsorption and desorption isotherms were measured using a Micromeritics ASAP 2020M system.

1.5 Gas sensing investigation

Gas sensors were fabricated by the conventional method.¹ The ZnO powder was ground with water to form the viscous slurry, and then the viscous slurry was coated onto the Al₂O₃ ceramic tubes with a pair of Au electrodes and four Pt wires. Finally, a Ni-Cr wire was inserted into the ceramic tube. The sensors were aging for about 3-7 days for further use. The gas-sensing performances of the sensors were elucidated using ethanol, methanol and formaldehyde as testing gases. Gas sensing tests were performed on a commercial CGS-8 (Chemical Gas Sensor-8) gas sensing measurement system (Beijing Elite Tech Company Limited) with a static gas distributing system (1 L). After the resistance of the sensor was stable at the tested temperature, pure target gas was injected into the gas bottle using a micro-injector. After the sensor resistance reached a new stable value, the gas bottle was opened and the sensor was then put into another empty bottle. The response value (R) was designated as $R = R_a/R_g$, where R_a was the base resistance of the sensor in air and R_g was the resistance of the mixture gases composed by target gas and air. The time taken by the sensor resistance changes from R_a to $R_a - 90\% \times (R_a - R_g)$ was defined as response time when the target gas was introduced to the sensor, and the time taken from R_g to $R_g + 90\% \times (R_a - R_g)$ was defined as recovery time when the ambience was replaced by air.

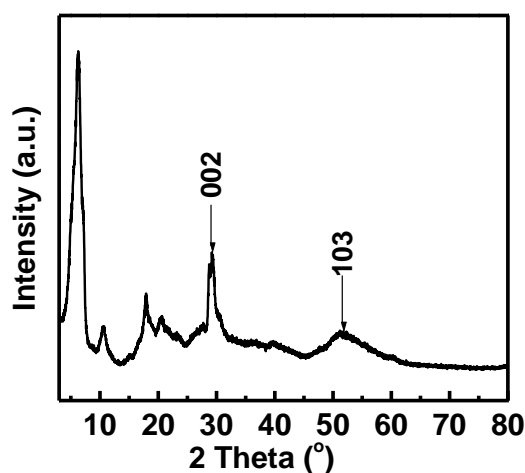


Fig. S1. XRD pattern of ZnS-CHA.

The peaks at $2\theta = 29.4$ and 51.8° are attribute to be the wurtzite ZnS. The presence of these XRD peaks ($2\theta < 20^\circ$) may due to the assembly behavior of CHA in the previous report.²

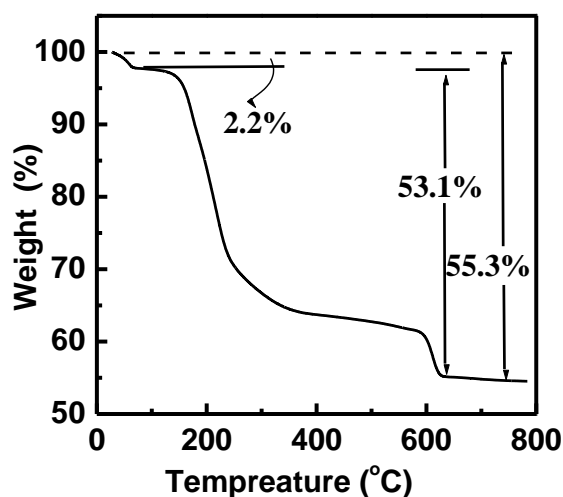


Fig. S2. TG analysis of ZnS-CHA nanocomposite in air.

The first weight loss in the range of 30 to 66 °C accompanying with a weight loss of 2.2%, owing to the loss of water weekly absorbed on the precursor. Then a great weight loss of 55.3% occurred at 130 °C and ended at 630 °C which can be attributed to the decomposition of the organic components in the precursor.

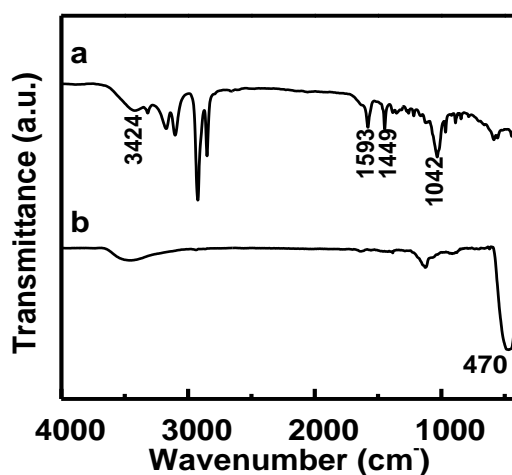


Fig. S3. IR spectra of (a) ZnS-CHA and (b) ZnO.

The peak located at 470 cm⁻¹ can be attributed to the intrinsic absorption of ZnO.³

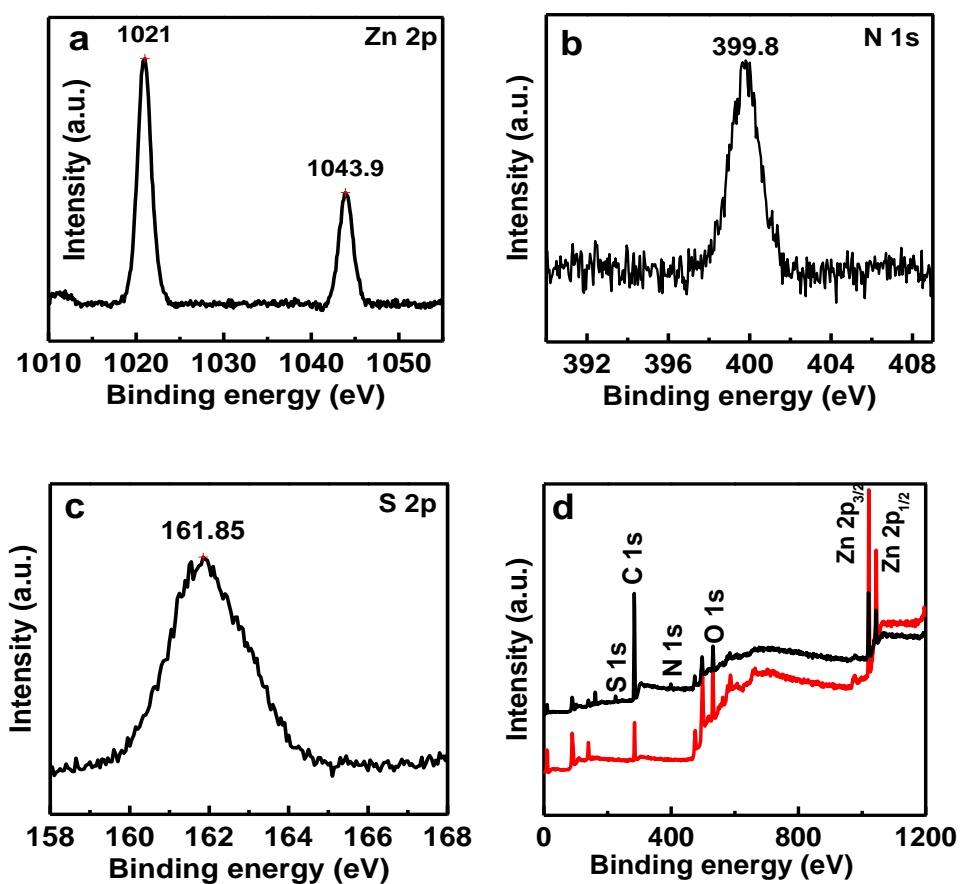


Fig. S4. High-resolution XPS survey spectrum of ZnS-CHA: (a) Zn 2p, (b) N 1s and (c) S 2p and (d) the wide-scan spectrum survey of the precursor and the obtained ZnO nanotubes calcined at 500 °C (red line).

There are two peaks of Zn 2p which are located at 1021 and 1043.9 eV, respectively. S 2p shows one peak at 161.8 and N 1s exhibits the peak at 399.8 eV. The binding-energy value of N 1s is nearly the same as that of alkylamine (399.6 eV).⁴ It indicates that the CHA molecules in the ZnS-CHA nanocomposite exist only in the form of -NH₂, which is in agreement with the observation in IR spectrum (Fig. S3†).

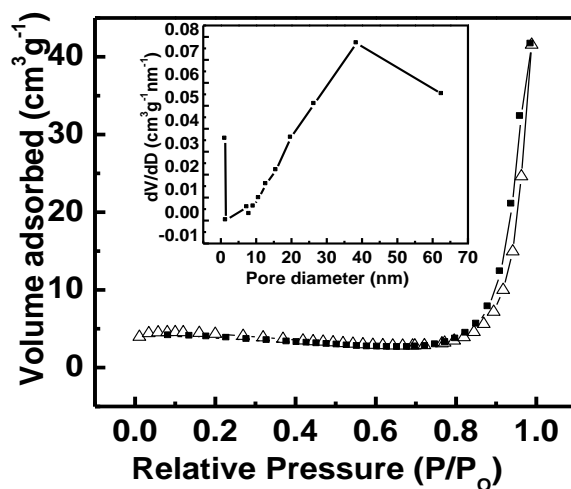


Fig. S5. Nitrogen adsorption-desorption isotherm and pore size distribution plots inset of porous ZnO nanotubes.

The BET surface area of the porous ZnO nanotubes is calculated to be 14 m²g⁻¹. Such low BET surface area is similar as many other reported nanomaterials, and can be understood by considering its large pore diameter.⁵

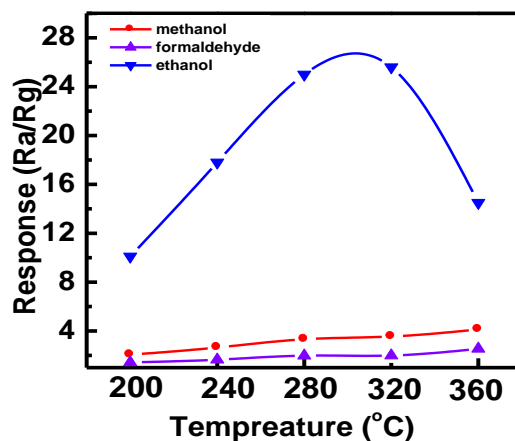


Fig. S6. Temperature-response relationships of the obtained ZnO nanotubes sensor to ethanol, methanol and formaldehyde.

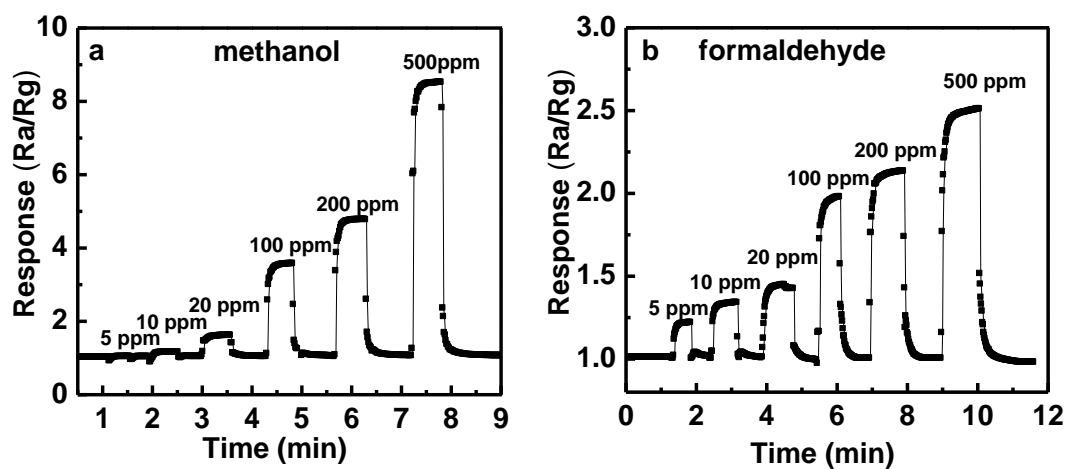


Fig. S7. Response-recovery curves of the sensor based on the ZnO nanotubes to (a) methanol and (b) formaldehyde.

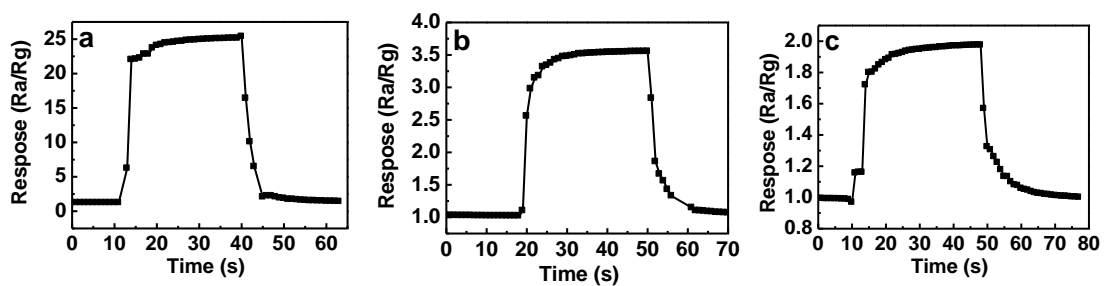


Fig. S8. Response-recovery curves of the sensor based on the ZnO nanotubes to 100 ppm (a) ethanol, (b) methanol and (c) formaldehyde.

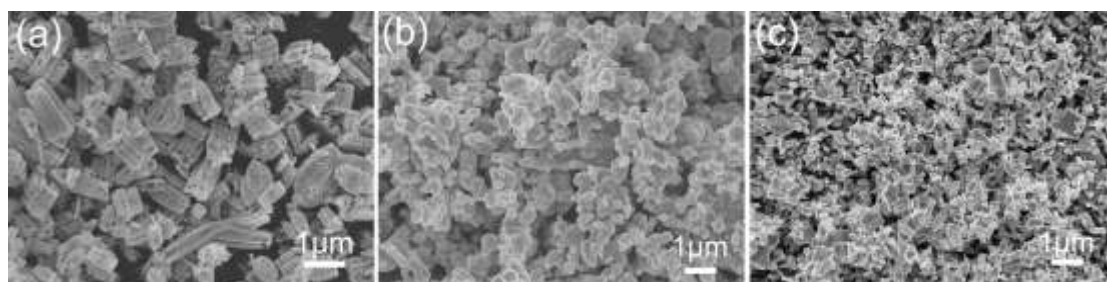


Fig. S9. SEM images of the (a) ZnO nanotubes obtained at 500 °C, (b) ZnO powder obtained at 750 °C and (c) commercial ZnO material.

Reference

1. L. Liu, S. C. Li, J. Zhuang, L. Y. Wang, J. B. Zhang, H. Y. Li, Z. Liu, Y. Han, X. X. Jiang, P. Zhang, *Sens. Actuators B Chem.*, 2011, **155**, 782-788.
2. X. X. Zou, G. D. Li, J. Zhao, P. P. Wang, Y. N. Wang, L. J. Zhou, J. Su, L. Li, J. S. Chen, *Inorg. Chem.*, 2011, **50**, 9106-9113.
3. Y. Yang, Y. Chu, Y. P. Zhang, F. Y. Yang, J. L. Liu, *J. Solid State Chem.*, 2006, **179**, 470-475.
4. Q. S. Gao, P. Chen, Y. H. Zhang, Y. Tang, *Adv. Mater.*, 2008, **20**, 1837-1842.
5. J. Y. Liu, Z. Guo, F. L. Meng, T. Luo, M. Q. Li, J. H. Liu, *Nanotechnol.*, 2009, **20**, 125501.